SIMULATION OF THE GRID IMPACTS OF A DISTRIBUTED PV FLEET

LISA GROSSI(1) • GEORG WIRTH(1)• ANDREAS SPRING(1) • GERD BECKER(1) • ROBERT PARDATSCHER(2) • ROLF WITZMANN(2) • JOHANNES BRANTL(3) • SEBASTIAN SCHMIDT(3)

(1) University of Applied Sciences Munich · Department of Electrical Engineering · 80335 Munich · Germany · Phone +49 (0) 89 1265-4412 · lgrossi@hm.edu
(2) Technische Universität München · Department of Electrical Engineering and Information Technology - Associated Institute of Power Transmission Systems · 80290 Munich
(3) Bayernwerk AG · Assetmanagement · 93049 Regensburg

ABSTRACT: In Southern Germany increasingly photovoltaic (PV) plants feed into the grid. New load patterns occur and with them changed grid requirements. In order to maintain grid stability and safety, the network operator needs detailed knowledge of the condition of the grid. This paper presents a simulation model that allows to model the feed-in power of the distributed PV fleet and to characterize the consumption in the medium and low voltage grid of the investigated area. The simulation bases on irradiance and temperature data recorded by a spatially distributed high resolution measurement system. The number of measurement devices used as simulation input and the time resolution of the input data are varied. The impact of the variation on the simulation accuracy is discussed.

Keywords: Grid-Connected, Grid Integration, Grid Stability, Grid Management

1 INTRODUCTION

The increasing share of renewable energies in the German power supply leads to changed grid requirements that must be met by the network operator to maintain grid stability and safety [6]. In this context Bayernwerk AG has initiated the project "Netz der Zukunft" ("Grid of the Future") in cooperation with the University of Applied Sciences München and Technische Universität München. It examines the impact of photovoltaic (PV) systems on the grid.

For this purpose, power quality measurements are carried out at about 700 metering points in a project area. The instruments are installed at every substation (110-20 kV and 20-0.4 kV) and at many house connections with and without PV power plants. All measurement devices transfer the data to a centralized database.

The project area is situated in a rural area in Northern Bavaria and characterized by a very high PV penetration. Altogether 36 MW of PV capacity are installed in the low and medium voltage grid. This amounts to ca. 5.6 kW per house connection.

In order to determine the behaviour of the distributed PV fleet, the spatial distribution of the irradiation in the investigated area is analysed. A special focus thereby is to characterize the geographic smoothing of the feed-in power on days with fluctuating cloud covers. Therefore, a high resolution measurement system records global irradiation and temperature. Figure 1 illustrates the positions of the measuring points in the investigated area. The distributed fleet and the measurement stations are spread over an area of ca. 11x15 km. Additionally, highly resolved grid measurements are available. The acquired data is being used to simulate the power generation of the distributed PV fleet.

On the basis of the simulation it is possible to analyse the effects of various meteorological conditions on the distribution network and identify critical weather situations. Further on, it enables the network operator to predict the feed-in power of the distributed PV fleet and to gain detailed knowledge on the behaviour and condition of the distribution network. This can serve as basis for feed-in management and regulatory measures.

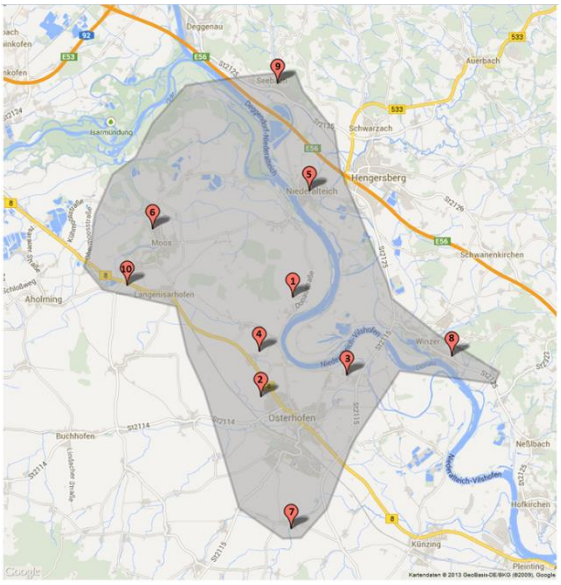

Figure 1: Positions of the measuring points in the project area.

2 SIMULATION APPROACH

The project area is divided into ten subareas of which each is simulated separately. The simulation model is efficiency-based and uses a PT1 element to model the geographic smoothing of the feed-in power on days with fluctuating cloud covers. Its time constant depends on the installed PV capacity of the corresponding subarea. The approach is similar to the one presented in [2]. Figure 2 illustrates the schematic of the simulation process.

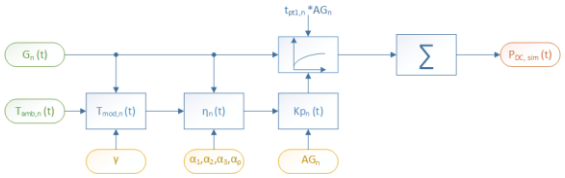

Figure 2: Schematic of the simulation process. Each subarea is simulated separately.

The following variables are used as input: The spatially distributed measurement devices record global horizontal irradiance and ambient temperature. First, horizontal irradiance is converted into global tilted irradiance using the model presented in Perez *et al.* [3]. Then, by means of the recorded ambient temperature, tilted irradiance and the module-specific parameter γ, the module temperature is calculated:

$$T_{mod} = T_{amb} + \gamma G_{tilt} \quad (1)$$

The parameter γ depends on the mounting type of the PV plant [1].

In the next step module efficiency η is determined:

$$\eta = (\alpha_1 + \alpha_2 G_{tilt} + \alpha_3 \ln(G_{tilt}))(1 + \alpha_p(T_{mod} - 25°C)) \quad (2)$$

with the parameters $\alpha_1, \alpha_2, \alpha_3$ describing the part load behaviour of the modules for a module temperature of 25°C. The parameters depend on the cell type. The parameter α_p corresponds to the temperature coefficient and describes the module behaviour at module temperature $T_{mod.}$ For the simulation model, weighted average values of $\alpha_1, \alpha_2, \alpha_3$ and α_p representing the different cell types on the market are used.

Module efficiency η and the installed PV capacity *AG* determine the proportional gain K_p. The time constants have been empirically determined and optimized in [5] on the basis of highly resolved data of the PV plants "Messedach Riem" and "Rothenburg" in Germany in dependency of the installed PV capacity. Proportional gain K_p and the time constant t_{pt1} are the input parameters of the PT1 element. Its output is the DC power of the single subareas and finally the power of the whole distributed PV fleet.

$$P_{DC,n}(t) = t_{pt1,n}\left(K_{p,n} * G_n(t) + P_{DC}(t\text{-}1)\right) + P_{DC}(t\text{-}1) \quad (3)$$

$$P_{DC,sim}(t) = \sum_{n=1}^{10} P_{DC,n}(t) \quad (4)$$

DC power is converted into AC power using the model presented by Schmidt and Sauer [4]. Additionally, system losses of 9.5% are considered [1]

On the basis of the simulated feed-in power and the cumulated power of the area measured over the 110 kV substation, that we have at our disposal, a reference load can be calculated. The load curve is calculated for a clear sky day and serves as reference for the simulation of further days. Figure 3 illustrates the simulated feed-in power, the measured load curve and the resultant calculated reference load.

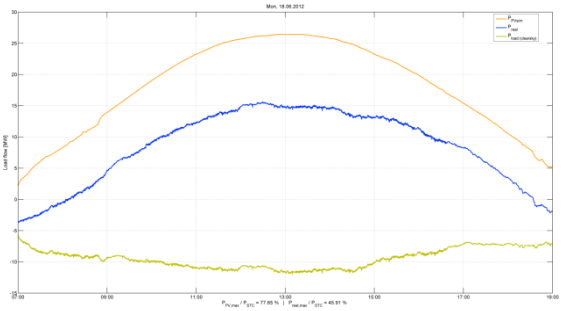

Figure 3: Simulated feed-in power (orange), cumulated power of the area measured over the 110 kV substation (blue) and calculated reference load (green) on 18 June 2012.

3 VALIDATION OF THE MODEL

Figure 4 illustrates a simulation result on the basis of just one measurement device. The accuracy of the simulation is indicated by the congruence between the dark and the light blue curve. It can be seen that simulation and real measured data match rather well for a clear sky. For fluctuating sky conditions the simulation differs from the measured power.

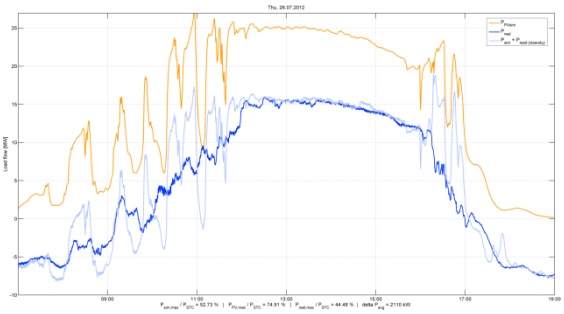

Figure 4: Simulation of the power generated by the distributed PV fleet (orange), measured (dark blue) and calculated (light blue) cumulated power of the area on 26 July 2012. The congruence between the dark and the light blue curve indicates the accuracy of the simulation. Only one measurement station is used as simulation input. Simulation and real measured data match rather well for a clear sky.

Figure 5 shows the simulation of a day with continuously fluctuating cloud cover based on just one station. The strongly fluctuating course of the load curve cannot be represented and the ratio P_{PVmax}/P_{STC} is 94.59%.

Figure 6 illustrates the same day simulated on the basis of the above described schematic using all ten measurement devices as input. Each subarea is simulated separately and described by its respective time constant. A better match between measurement and simulation is visible. The ratio P_{PVmax}/P_{STC} of 72.77% represents the smoothing effect.

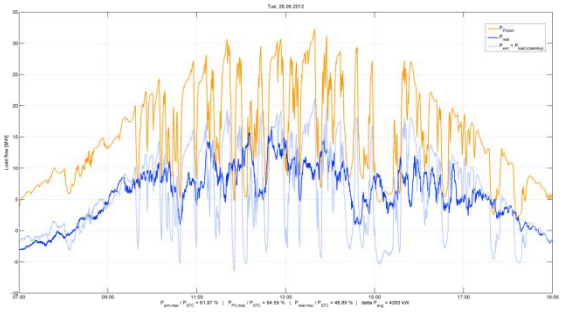

Figure 5: Simulation of the power generated by the distributed PV fleet (orange), measured (dark blue) and calculated (light blue) cumulated power of the area on 26 June 2012. Only one station is used as simulation input.

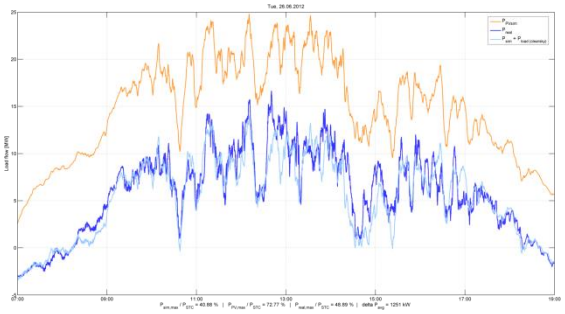

Figure 6: Simulation of the power generated by the distributed PV fleet (orange), measured (dark blue) and calculated (light blue) cumulated power of the area on 26 June 2012. Ten stations are used as simulation input.

Since the rmse alone does not reflect the congruence between the courses of the two curves to be compared, additionally the ramp rate is introduced. It can be seen that the ramp rates of the feed-in power simulated on the basis of just one measurement station are remarkably higher than on the basis of all ten stations. On 26 June 2012 the single device shows a maximum power ramp rate ΔP referred to the installed PV capacity of 36 MW of 51.9% in 50 seconds. 99% of the simulated data points are situated below a straight line with a slope of 1.2 % per second. Using all ten stations the simulated feed-in power features a maximum $\Delta P/P_{inst}$ of just 23.98% in 50 seconds. The straight line's slope amounts to 0.22% per second.

Table 1 contains statistical values on the simulation accuracy. 20 days with various cloudiness conditions have been analysed. The root mean square error refers to the overall installed PV capacity of ca. 36 MW in the area. Maximum and minimum rmse and average absolute deviation (aad) values are indicated. The mean rmse amounts to 2.37 % and the aad to 1.23 MW.

$$\mathrm{rmse} = \sqrt{\frac{1/\mathrm{N}\sum_{\mathrm{i}=1}^{\mathrm{N}}(\mathrm{x_{meas}}\text{-}\mathrm{x_{sim}})^2}{{\mathrm{P_{inst}}}^2}} \qquad (5)$$

$$\mathrm{aad} = 1/\mathrm{N}\sum_{\mathrm{i}=1}^{\mathrm{N}}|\mathrm{x_{meas}} - \mathrm{x_{sim}}| \qquad (6)$$

Table 1: Statistical values describing the simulation accuracy.

Date (2012)	Root mean square error [%]	Average absolute deviation [MW]
01 June	2.11	1.05
02 June	3.14	1.52
03 June	1.65	0.80
04 June	2.80	1.55
05 June	2.63	2.49
07 June	4.45	2.60
09 June	3.16	1.71
11 June	2.36	1.14
13 June	3.02	1.61
15 June	1.55	0.77
19 June	0.97	0.46
20 June	1.80	0.89
21 June	2.46	1.19
22 June	2.34	1.11
25 June	2.86	1.40
26 June	2.66	1.22
28 June	1.61	0.74
01 July	2.04	1.02
04 July	2.17	1.01
21 Aug	1.63	0.44

Additionally, the simulated feed-in power has been validated by comparing it to the measurement data of the feed-in metering devices in the area. Depending on the day, between 150 and 200 PV measurements devices were available for the validation. Figure 7 shows an exemplary day. In general the two curves fit well. At noon the simulated feed-in power curve slightly exceeds the measured data. This is due to the fact that we convert horizontal to tilted irradiance assuming a slope of 30° for all PV plants in the area. 30° corresponds to the theoretical ideal slope value for PV plants situated in Germany.

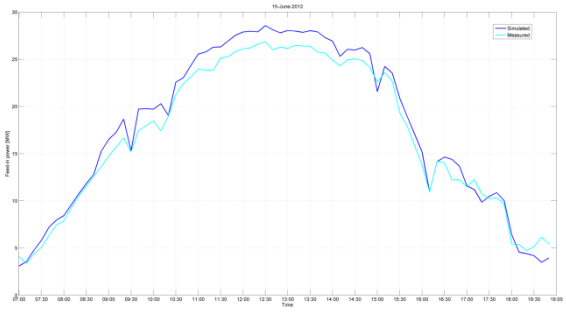

Figure 7: Comparison between the simulated (dark blue) and measured (light blue) feed-in power.

4 VARIATION OF THE NUMBER OF MEASUREMENT DEVICES AND THE TIME RESOLUTION

In order to estimate the optimal measurement density for operational products defined by the network operator, the number of measurement devices is varied from one to ten. The dependency of the simulation accuracy on the number of measurement devices used as simulation input is examined. Figure 8 shows the principle.

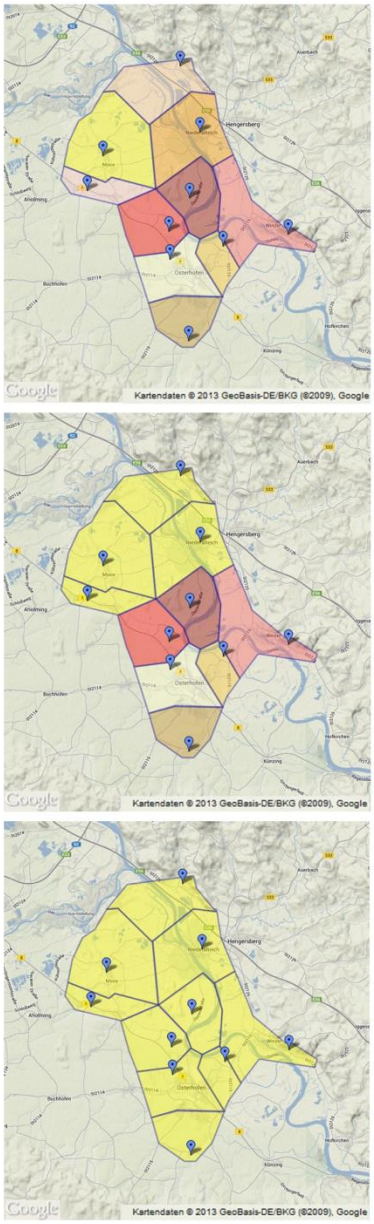

Figure 8: In the first simulation step all ten subareas are simulated separately. Then, the subareas are merged one after another. New areas sizes and time constants arise. In the last step the whole investigation area is simulated with only one measurement station.

Nine days are simulated in four different variants of merging the single measurement devices. Only these nine days in June are chosen as representative days due to irregularities in the data set caused by switching operations in the investigated grid. In this way only surely reliable data is used for the analysis. Additionally, the time resolution is varied and the simulation is carried out with resolutions of 1 second, 1 minute, 10 minutes, 15 minutes and 60 minutes. Hence, a total of 1800 data points are created.

Figure 9 illustrates the root mean square error (rmse) as a function of the number of measurement devices on the x-axis and the time resolution on the y-axis. The grey points correspond to all simulated values and the surface is gained by biharmonic interpolation of their mean values. As mentioned above, the rmse values are given in percent and refer to 36 MW.

For reasons of clarity, figure 10 depicts the same content as contour plot. Each colour corresponds to one percent of the rmse colour scale. In this way it is easy to get an overview of the course of the rmse along the x-axis and the y-axis in order to read out rmse values.

It can be seen that the time resolution has only minor impact on the accuracy. The rmse remains rather constant along the y-axis. The crucial variable is the number of stations. Rmse decreases distinctly with increasing number of measurement devices used as simulation input, especially between one to three stations where four colour ranges occur. From three measurement devices used as simulation input the colour ranges become wider. Their width corresponds approximately to two devices.
Since the number of measurement stations is the determining variable, for each number of devices the rmse values of all time resolution, nine days and four variants are averaged. Then the slope of the course of the averaged values is calculated. The strongest decline occurs in the range between one to three stations. Rmse falls with a slope of ca. 1.5 % per station from 9.48 % to 6.55 % on average. In the range between three to nine stations rmse drops with a mean value of 0.49 % per station. From nine to ten stations the slope amounts just to 0.34 %.

5 CONCLUSION

The presented simulation model allows us to determine the behaviour of the spatially distributed PV fleet in the investigation area. On its basis it is possible to analyse the effects of various meteorological conditions on the distribution network and identify critical weather situations. The simulation on the basis of just one measurement device is sufficient for clear sky days. To visualize the geographic smoothing of the feed-in power on days with fluctuating cloud covers, additional metering points are necessary. Figures 5 and 6 show that, due to the smoothing effect, a distributed fleet features a lower P_{PVmax}/P_{STC} ratio than a single PV system.

The number of measurement devices used as simulation input is the crucial factor determining the simulation accuracy. Time resolution has only minor impact. In the range between one to three devices the accuracy decreases the strongest from 9.48% to 6.55. From the third measurement station the colour ranges correspond approximately to two stations.

On the basis of the presented results, the network operator is able characterize the condition of the grid. Further on, the simulation accuracy can be adapted to the requirements of the operational management. Consequently, the network operator is able to take regulating measures to ensure quality and security of supply.

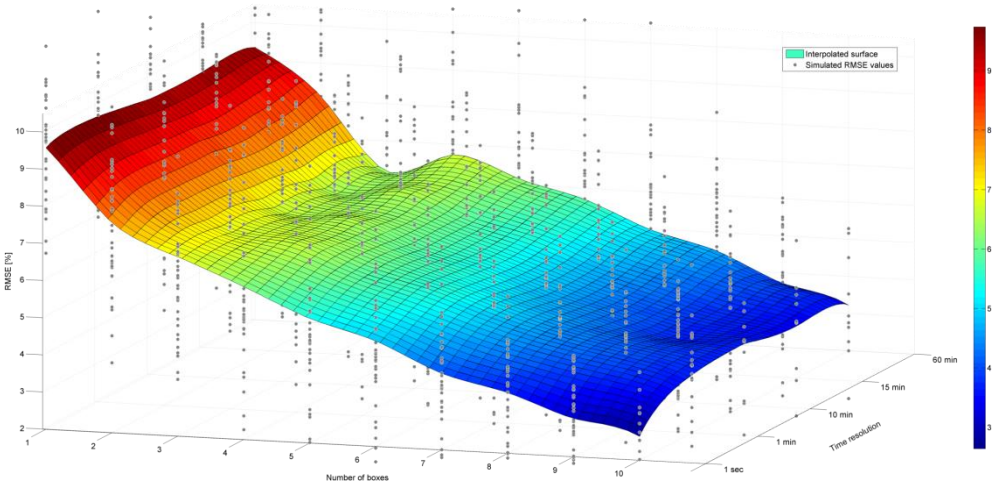

Figure 9: Three dimensional plot of the root mean square error as a function of the number of measurement stations on the x-axis and the time resolution on the y-axis. The grey points correspond to all simulated values and the surface is gained by interpolation.

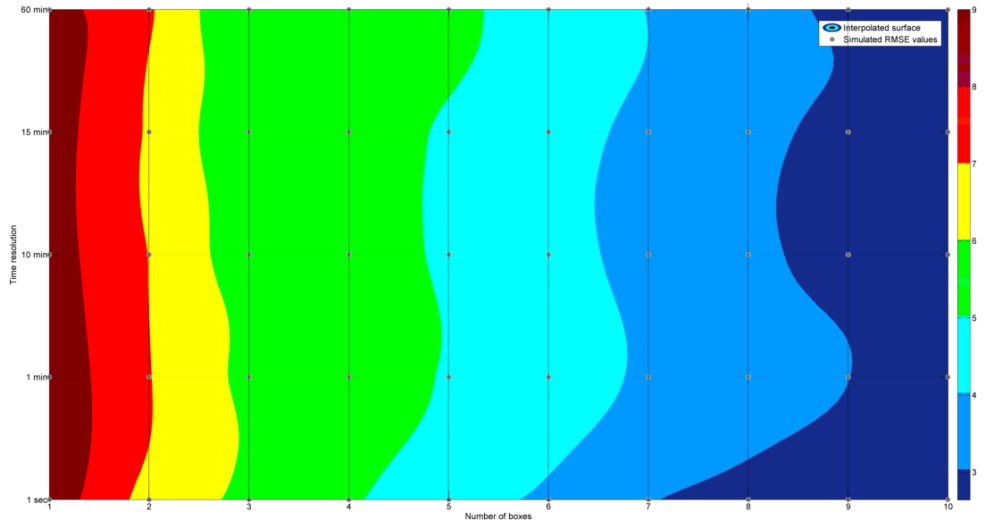

Figure 10: Contour plot of the root mean square error as a function of the number of measurement stations on the x-axis and the time resolution on the y-axis.

[1] Lorenz E., Scheidsteger T., Hurka J., Heinemann D., Kurz C., Regional PV power prediction for improved grid integration, Progress in Photovoltaics, Special Issue: 25th EU PVSEC WCPEC-5, Valencia, Spain, 2010, Volume 19, Issue 7, pages 757–771, November 2011.

[2] Marcos J., Marroyo L., Lorenzo E., Alvira D., Izco E., From irradiance to output power fluctuations: the pv plant as a low pass filter. Prog. Photovolt: Res. Appl. 2011: 19: 505–510

[3] Perez R., Seals R., Ineichen P., Stewart R., Menicucci D., A new simplified version of the Perez diffuse irradiance model for tilted surfaces. Solar Energy 1987: 39: 221-231.

[4] Schmidt H, Sauer DU.,Wechselrichter-Wirkungsgrade. Sonnenenergie 1996; 4: 43–47 (in German).

[5] Stauner V., Identifikation der Übertragungszeitkonstanten von Photovoltaiksystemen, Bacherlorarbeit, Hochschule München, April 2012.

[6] Wirth G., Spring A., Becker G., Pardatscher R., Witzmann R., Brantl J., Garhamer M., Effects of a High PV Penetration on the Distribution Grid. 27th European Photovoltaic Solar Energy Conference and Exhibition, Frankfurt, September 2012.